Synthetic gene circuits enable systems-level biosensor discovery at the host-microbe interface

Running title: Synthetic gene circuits enable gut biosensor discovery

Authors

Alexander D Naydich[1,2], Shannon N Nangle[1,2], Johannes J Bues[1], Disha Trivedi[1], Nabeel Nissar[1], Mara C Inniss[1], Matthew J Neiderhuber[1], Jeffrey C Way[2], Pamela A Silver[1,2]# & David T Riglar[1,2]#

Affiliations

1. Department of Systems Biology, Harvard Medical School, Boston, MA 02215

2. Wyss Institute for Biologically Inspired Engineering, Boston, MA 02215

Corresponding author email: David_Riglar@hms.harvard.edu and Pamela_Silver@hms.harvard.edu

Abstract word count: 348

Text word count (excluding the references, table footnotes, and figure legends): 4912

Present addresses: J.J.B.: Laboratory of Systems Biology and Genetics, EPFL-SV-IBI-UPDEPLA, Station 19, AI 1240, CH-1015 Lausanne, Switzerland; N.N.: Littleton MA, 01460; M.C.I.: Obsidian Therapeutics, 1030 Massachusetts Avenue, Suite 400, Cambridge MA, 02138; M.J.N.: McKay Lab at UNC Chapel Hill, 3344 Genome Sciences Building, Campus Box 3280, Chapel Hill, NC 27599.

ABSTRACT

The composition and function of the gut microbiota are strongly associated with human health, and dysbiosis is linked to an array of diseases, ranging from obesity and diabetes to infection and inflammation. Engineering synthetic circuits into gut bacteria to sense, record and respond to *in vivo* signals is a promising new approach for the diagnosis, treatment and prevention of disease. Here, we repurpose a synthetic bacterial memory circuit to rapidly screen for and discover new *in vivo*-responsive biosensors in commensal gut *Escherichia coli*. We develop a pipeline for rapid systems-level library construction and screening, using next-generation sequencing and computational analysis, which demonstrates remarkably robust identification of responsive biosensors from pooled libraries. By testing both genome-wide and curated libraries of potential biosensor triggers—each consisting of a promoter and ribosome binding site (RBS)—and using RBS variation to augment the range of trigger sensitivity, we identify and validate triggers that selectively activate our synthetic memory circuit during transit through the gut. We further identify biosensors with increased response in the inflamed gut through comparative screening of our libraries in healthy mice and those with intestinal inflammation. Our results demonstrate the power of systems-level screening for the identification of novel biosensors in the gut and provide a platform for disease-specific screening using synthetic circuits, capable of contributing to both the understanding and clinical management of intestinal illness.

IMPORTANCE

The gut is a largely obscure and inaccessible environment. The use of live, engineered probiotics to detect and respond to disease signals *in vivo* represents a new

42 frontier in the management of gut diseases. Engineered probiotics have also shown
43 promise as a novel mechanism for drug delivery. However, the design and construction
44 of effective strains that respond to the *in vivo* environment is hindered by our limited
45 understanding of bacterial behavior in the gut. Our work expands the pool of potential
46 biosensors for the healthy and diseased gut, providing insight into host-microbe
47 interactions and enabling future development of increasingly complex synthetic circuits.
48 This method also provides a framework for rapid prototyping of engineered systems and
49 for application across bacterial strains and disease models.

INTRODUCTION

Recent advances in our understanding of both the human microbiota and biological engineering techniques have created myriad possibilities for the development of synthetic microbes for *in vivo* clinical applications (1, 2). Bacteria residing in the gut are uniquely positioned to monitor a variety of host, microbial, and environmental factors and to respond to changes in intestinal homeostasis. Engineered gut bacteria also offer the potential for *in vivo* production and delivery of therapeutics (2).

Environment- and disease-responsive functions, which could minimize both the metabolic burden of engineered systems on the bacteria and off-target effects on the patient, offer exciting prospects for clinical applications. To this end, recent *in vivo* approaches have developed sensors responding to inflammation (3, 4), intestinal bleeding (5), and pathogen quorum-sensing systems (6, 7). However, the construction of disease-responsive circuits in bacteria has been hindered by the limited number of characterized bacterial systems that can be reliably employed as sensors.

Mining the genomes of native gut bacteria is a promising approach for discovering new sensors that respond under conditions of interest, such as in the healthy or diseased gut. To date, these efforts have largely relied on transcriptome sequencing and proteomics of fecal samples. However, to obtain an instantaneous snapshot of bacterial behavior inside the gut using these techniques, invasive sampling is required (i.e., colonoscopy and biopsy). Furthermore, transient or low-abundance signals may not be detected, and any responsive genetic elements identified with these techniques may not function predictably when employed in synthetic circuits. Approaches such as *in vivo* expression technology (IVET) and recombinase-based

IVET (RIVET) have also been used to track *in vivo*-expressed genes non-invasively, but detect only constitutive expression (for IVET) and may have high false-positive rates (8). Nevertheless, these technologies show the potential for systems-level approaches to interrogate the behavior of the microbiota.

We have previously developed an approach for non-invasive measurement of bacterial responses in the gut, based on a robust synthetic memory circuit, which records environmental stimuli via a transcriptional trigger (3, 9). When activated, the trigger turns on a memory switch, which can retain the memory-on state for over a week in the gut (9). After the bacteria pass through the host, their memory state can be determined via reporter gene expression, enabling non-invasive readout of transient signals within the gut. The circuit can maintain functional and genetic stability during six months' colonization of the mouse gut, demonstrating its suitability for longitudinal studies and its potential to support the development of stable, engineered biosensors for *in vivo* deployment (3).

Here, we adapt this memory circuit for parallel, high-throughput screening of hundreds of potential triggers. We apply this method to identify new biosensors responding specifically to the *in vivo* gut environment. Through comparison between healthy mice and those suffering from inflammation, we also identify triggers that respond differentially during disease. Together, these results provide a platform for *in vivo* non-invasive biosensor discovery and longitudinal testing.

RESULTS

Bacterial memory as a biosensor screening tool. To enable screening of new potential biosensors in parallel, we modified our previously-developed *E. coli* memory circuit, which is based on the λ phage lysis–lysogeny switch (Fig. S1A) (9). This modified circuit is referred to as the high-throughput memory system (HTMS) (Fig. 1A). Both the original memory circuit and the HTMS consist of a trigger—based on a transcriptional promoter activated in the presence of a certain stimulus—and a memory switch. The memory-on and memory-off states of the switch correspond to the mutually-repressive proteins Cro and CI, respectively. Additionally, a β-galactosidase (LacZ) reporter is produced in the memory-on state.

One key modification for the HTMS is the triggering of memory using a dominant-negative mutant of the *cI* gene (*cIDN*), instead of *cro* used in the original trigger. When the trigger promoter is activated by a stimulus, CIDN monomers, which have an N55K mutation in the DNA binding region (10) dimerize with wild-type (WT) CI monomers expressed in the memory-off state, creating heterodimers that are deficient in DNA-binding. This leads to derepression of P_R and transition to the memory-on state. As with the CI used in the memory element, CIDN carries a mutation to prevent RecA-mediated cleavage (ind-) (11).

Use of CIDN in the trigger ensures that there is no delay of switching to the memory-on state in the case of high, or constant, expression of the trigger promoter. To test this, a P_{tet} trigger driving *cIDN* or *cro* was integrated into *E. coli* K-12 MG1655 and NGF-1 strains containing a memory element. When grown in the presence of a high concentration (100 ng/ml) of anhydrotetracycline (aTc) inducer, *cIDN*-triggered strains

showed switching to the memory-on state, while *cro*-triggered strains switched only after a subsequent period of growth in the absence of aTc (Fig. 1B).

The original memory circuit expresses a *lacZ* reporter gene for screening on indicator plates (9). To analyze pooled libraries containing many strains with varied trigger promoters, the HTMS also expresses a spectinomycin-selectable resistance gene (*aadA)* in the memory-on state.

This antibiotic-selectable memory maintains response characteristics similar to the original memory element. To test this, a P_{tet} trigger driving *cIDN* was integrated into strains containing *lacZ* (original) or *aadA*+*lacZ* (HTMS) memory elements, creating PAS809 and PAS810, respectively (see Table 1 for strain list). Strains were induced by aTc (0-100 ng/ml) and the response quantified by plating cultures on indicator plates containing 5-bromo-4-chloro-3-indolyl-β-d-galactopyranoside (X-gal), which turns blue in the presence of LacZ, indicating a memory-on state (Fig. S1B). Both strains responded similarly to aTc (*original memory* EC50: 4.1-4.6 ng/ml, 95% CI; *HTMS* EC50: 4.0-4.3 ng/ml, 95% CI), confirming the circuit's modularity to additional reporters in the memory-on state.

The HTMS allows faithful selection of memory-on colonies with spectinomycin treatment. Plating of fully memory-off, fully memory-on, and 50-50 mixed cultures of PAS810, on indicator plates with and without spectinomycin further demonstrated that all spectinomycin-selected colonies were also *lacZ* positive (Fig. 1C). Spectinomycin did not yield false-positive results by inducing memory switching (fully memory-off: 0% +/- 0% SE, n = 8), nor excessive false-negative results through inhibition of memory-on bacterial growth (fully memory-on: 93.0% +/- 4.2% SE, n = 8; 50-50 mix: 49.7% +/- 1.5%

SE, n = 5) (Fig. 1C). Together these results demonstrate the ability of the HTMS to measure biosensor response and allow selection for downstream pooled analyses.

Biosensor library construction. To build biosensor libraries for genomic integration, we adapted a Tn7 transposon genome insertion plasmid (12) for rapid Golden Gate assembly (13) of bacterial promoters upstream of the *cIDN* trigger and insertion into the genome of memory bacteria (Fig. 2A and S2). The modularity of this cloning strategy allows for adjustment of trigger sensitivity through incorporation of ribosomal binding site (RBS) variants, which vary the translation rate of mRNA transcripts (Fig. 2A). To test this concept, triggers consisting of a P_{tet} promoter combined with nine synthetic RBS sequences—previously demonstrated to vary widely in their translation strength (14) (Fig. 2A)—were constructed and inserted into the genome of HTMS bacteria, and the HTMS response to varying concentrations of aTc (0-100 ng/ml) was characterized (Fig. 2B). The RBS variants differed in their extent of memory induction at 0.1-10 ng/ml aTc (EC50 ranging from 0.5 to 4.1 ng/ml for responsive strains), illustrating our ability to tune trigger sensitivity.

We explored two approaches for generating biosensor libraries: 1) a genome-wide collection of trigger promoters that would enable screening of a bacterium's entire range of transcriptional responses (MG1655 library), and 2) a curated collection of promoters with sensitivity variants aimed at detecting inflammation (Nissle 1917 library). Both libraries were assembled into an HTMS-containing *E. coli* NGF-1 strain (PAS811), as NGF-1 has proven to be an efficient and persistent colonizer in the mouse gut (3, 9, 15). The genome-wide library was sourced from a previously published collection of 1600 unique promoters from *E. coli* K-12 MG1655 (16). Promoters and their wild-type

RBSs were amplified by PCR from this collection, assembled into our transposon plasmid, and integrated as triggers into the genome of PAS811. Because our method focuses on detecting off-to-on sensor transitions, the resultant library was further subsampled by pooling 500 colonies that were LacZ-negative under routine *in vitro* culture. Sequencing confirmed the presence of 155 unique strains in this final genome-wide library.

Our second library was constructed with a subset of promoters sourced from the human probiotic *E. coli* Nissle 1917, which are involved in anaerobic respiration of sulfur- or nitrogen-oxides or nitrate, produced by the gut epithelium during inflammation (17, 18). For each promoter, a trigger with its wild-type RBS, as well as with five different synthetic RBSs (MCD5, MCD10, MCD15, MCD17 and MCD23) (14) were included to tune sensitivity. Sequencing confirmed that the assembled library contained 61 unique strains out of 66 total designed constructs.

Parallel analysis faithfully reports biosensor response. To screen for biosensor response, HTMS libraries are exposed to a condition of interest (Fig. 3A), and put through a processing, sequencing and analysis pipeline (Fig. 3B). After exposure, HTMS bacteria are recovered and cultured. The initial culture is split into two and back-diluted, and one of the two new cultures is subjected to spectinomycin selection. Following selection, the trigger regions of both cultures are sequenced and analyzed to produce an odds ratio for each trigger promoter in the library, corresponding to that trigger's memory state. To calculate odds ratios, results are normalized to a positive normalization strain (PAS812) which remained in a memory-on state (Fig. 3B).

Pooled library analysis is predictive of the on/off state of HTMS bacteria. The Nissle 1917 library was cultured aerobically in liquid media and analyzed to obtain odds ratios as described above. Concurrently, individual strains from this library were grown on indicator plates to assess each strain's *in vitro* memory state directly. Both tests showed strong agreement, with strains that were LacZ-positive also displaying higher odds ratios (Fig. 3C). Receiver operating characteristic analysis confirmed efficient distinction between memory-on and memory-off states, with an odds ratio of approximately 0.02 delimiting the boundary (Fig. 3D). This confirmed our sequencing method as a reliable indicator of biosensor memory state.

Differential biosensor response in the healthy mouse gut. To screen for biosensor response to growth within the murine gut, the MG1655 library was administered to specific-pathogen free (SPF) mice by oral gavage (~10^7 bacteria/mouse), and fecal samples were collected over one (n=2) or seven (n=3) days. High library diversity was maintained in both experiments (92% and 82% of strains identified in gavage samples present at experiment endpoint, respectively). Analysis of HTMS strains recovered from gavage suspension and fecal samples identified 23 unique strains that responded specifically to growth within the gut (gavage: odds ratio < 0.02; fecal samples: $\geq$ 1 timepoint odds ratio $\geq$ 0.02 and $p < 0.05$) (Fig. 4A and 4B; Data Set S1 and S2). Five strains (containing ydiL, ydjL, gatY, gcvA and ubiG triggers) were detected in the memory-on state in at least 4 of 5 mice. The two most consistent responders (ydjL and ydiL triggers) were selected for follow-up testing.

To validate the response of the ydiL and ydjL triggers during gut transit, memory bacteria containing these triggers (ydiL: PAS813; ydjL: PAS814) or a promoterless *cIDN*

gene (negative control: PAS815) were administered to SPF mice as monocultures. Fecal samples were collected and analyzed over the subsequent five days. Culture on indicator plates demonstrated an absence of memory activation in all three strains prior to gavage. However, when recovered from fecal samples PAS813 and PAS814 colonies were consistently memory-on, confirming activation during gut transit (at Day 2, PAS813: 51% +/- 8% SE; PAS814: 30% +/- 4% SE; negative control: 0% +/- 0% SE; n = 3 per strain) (Fig. 4C).

The Nissle 1917 library was also screened to discover promoters responding in the healthy mouse gut. Testing of the Nissle 1917 library over five days following gavage (~10^7 bacteria/mouse) identified 11 strains that specifically responded to *in vivo* growth (Data Set S3). Ten of these, derived from three unique promoters (*ynfEFGH*, *torCAD*, and *yeaR-yoaG* operons) registered a memory-on state in the majority of timepoints and all mice tested (n=4) (Fig. 4D and 4E). Promoter response was similar during parallel analysis in the inflamed mouse gut (n = 4; see below and Fig. 5 for experimental details), further validating these results (Fig. S3 and Data Set S3).

RBS variation to adjust trigger sensitivity affects *in vivo* sensing capacity. Variation in sensor response based on trigger RBS was most notably observed with the *ynfEFGH* promoter: WT, MCD5 and MCD17 RBSs showed no response throughout the screening experiment, whereas MCD10, MCD15, and MCD23 registered as memory-on in 100%, 100% and 94% of timepoints, respectively. (Note: Nissle 1917 library strains are referred to below by an abbreviation consisting of the first gene of the operon from which they are derived and the number of their synthetic RBS. For instance, “ynfE15” denotes the trigger consisting of the *ynfEFGH* promoter with MCD15.) To validate these

findings, ynfE15 (PAS816), yeaRWT (PAS817), and ynfEWT (PAS818, used here as a negative control) strains were administered to SPF mice as monocultures, with memory status determined by culture on indicator plates (at Day 2, ynfE15: 99% +/- 1% SE; yeaRWT: 31% +/- 4% SE; ynfEWT: 0% +/- 0% SE; n = 3) (Fig. 4F). Of note, changing the ynfE trigger RBS from WT to MCD15 increased memory-on rate in the gut from 0% to nearly 100%.

Together these results demonstrate the ability for HTMS analysis to rapidly identify biosensors *in vivo* and the power of varying trigger sensitivity to tune the strength of biosensor response.

***In vitro* induction of *in* vivo-responding biosensor strains.** The Nissle 1917 library includes some promoters with previously characterized induction conditions. We tested induction of *ynfEFGH* promoter trigger memory strains, which derive from an operon known to respond to low nitrate (through repression by phosphorylated NarL), and anaerobic (through FNR activation) conditions (19). When grown anaerobically in rich media, PAS816 (ynfE15), produced a memory response (13.3% +/- 0.7% SE; n = 7). With added nitrate (20 mM), or in aerobic conditions, the response was zero (-O_2/+nitrate: 0% +/- 0% SE; n = 3; +O_2/+nitrate: 0% +/- 0% SE; n = 3; +O_2: 0% +/- 0% SE; n = 3) (Fig. 4G), consistent with previous literature reports of *ynfEFGH* promoter behavior (19). Additionally, no response was observed from PAS818 (ynfEWT) in any condition (n = 3), suggesting that it is less sensitive than PAS816 (ynfE15), consistent with our *in vivo* results. In addition to growth in rich media, strains were also cultured anaerobically in cecal contents. As in rich media with no inducer, only ynfE15 responded to growth in cecal media (3.7% +/- 0.9% SE; n = 3) (Fig. 4G).

Identification of disease-specific biosensors. To look for sensors responding differentially to disease, we compared the response of the Nissle 1917 library in healthy mice (n = 4; as previously displayed in Fig. 4D, 4E and S3, and Data Set S3) to a murine intestinal inflammation model (Fig. 5A, 5B and S4, and Data Set S3). After library gavage, SPF mice were provided water containing 4% w/v dextran sulfate sodium (DSS) *ad libitum* for five days, and HTMS analysis was performed on fecal samples throughout. Weight loss (Fig. S4A), colon length reduction at endpoint (Fig. S4B), and increased *E. coli* CFU counts (Fig. S4C) were all consistent with increasing inflammation throughout the experiment. Six strains registered memory-on at more timepoints in the DSS-treated group than in the control group (Fig. 5A and 5B). In particular, the ynfE17 trigger strain (PAS819) responded specifically in DSS-treated mice (control: no response; DSS-treated: 93% of timepoints with odds ratio ≥ 0.02 and $p < 0.05$) (Fig. 5A and 5B, and Data Set S3).

To validate ynfE17 (PAS819) response to inflammation, the strain was administered to SPF mice as a monoculture, after which a subset of the mice was provided water containing 4% DSS. Fecal samples were cultured for memory bacteria on indicator plates for 7 days following gavage. As above, body weights (Fig. S4D), post-dissection colon lengths (Fig. S4E) and CFU counts of HTMS bacteria (Fig. S4F) reflected increased inflammation in DSS-treated mice. Confirming the screen results, ynfE17 showed increased response in DSS-treated mice compared to untreated controls, with the greatest difference between groups at days 6 and 7 (at Day 6, +DSS: 24% +/- 9% SE, n= 4; control: 5% +/- 2% SE, n = 8) (Fig. 5C). The strong response of PAS819 in the absence of DSS in one of the control group mice indicates that *in vivo*

277 conditions other than DSS treatment can activate the ynfE17 trigger. *In vitro* anaerobic
278 growth both in rich media and in cecal media did not induce ynfE17 (0 +/- 0% SE; n = 7;
279 0 +/- 0% SE, n = 3, respectively), in contrast to ynfE15 (Fig. 4G), suggesting a lower
280 nitrate threshold for ynfE17 activation and that individual bacteria may experience low
281 nitrate conditions within the inflamed mouse gut.
282

283 ## DISCUSSION

284 Here, we have expanded the use of a robust genetic memory circuit to assess
285 the *in vivo* responses of multiple bacterial sensors in parallel. The original memory
286 circuit (9) was altered to allow off-to-on transitions in the presence of constant induction,
287 and to enable selection of memory-on strains from pooled libraries using spectinomycin.
288 We developed a screening, sequencing and analysis pipeline to efficiently identify *in*
289 *vivo*-responding trigger–RBS combinations. Tests conducted with both genome-wide
290 and curated libraries containing hundreds of sensors demonstrated that our method is
291 an effective, non-invasive way to identify new biosensors responding in the gut. We
292 identified and validated biosensors responding to growth in the healthy mouse gut and
293 preferentially in inflamed conditions. Together, these results demonstrate the power of
294 tuning trigger sensitivity to physiological responses and for the HTMS to assess unique
295 features of the mammalian gut environment *in vivo*.
296 One advantage of our method is its ability to discover sensors that could not be
297 rationally designed based on existing knowledge, presenting an opportunity to apply the
298 rapidly increasing but largely uncharacterized genetic diversity identified through
299 microbiome sequencing. For instance, the two validated healthy-gut sensors from our *E.*

coli MG1655 library (PAS813 and PAS814) are derived from operons with largely uncharacterized function and regulation. PAS814 is triggered by the promoter of the *ydjLKJIHG* operon, which putatively includes a kinase, a transporter protein, two dehydrogenases, an aldolase and an aldo-keto reductase. Only the activity of the aldo-keto reductase, YdjG, has been confirmed through reduction of methylglyoxal (20, 21). Interestingly, a previous analysis of *E.coli* protein expression in germ-free mice showed that YdjG was expressed 3.5-fold higher in the cecum than *in vitro* (22). Another gene which has been studied in this operon, *ydjK*, may play a role in osmotolerance, showing a 50% increased growth rate in high-salt media when overexpressed in *E. coli* (23). It is not known whether methylglyoxal or osmotic stress can directly trigger transcription of the *ydjLKJIHG* operon. However, methylglyoxal occurs in many foods and is also produced by intestinal bacteria (24); it can also inhibit bacterial growth, suggesting a possible motivation for expression of *ydjLKJIHG* in the gut.

Promoters derived from three unique Nissle 1917 operons (*ynfEFGH*, *torCAD*, and *yeaR-yoaG*) showed robust memory response in the healthy mouse gut (Fig. 4D and 4E). The *ynfEFGH* operon encodes a DMSO reductase which has also been shown to reduce selenate (25, 26). It is activated by FNR in anaerobic conditions and repressed by phosphorylated NarL in the presence of nitrate (19), which was further confirmed by our *in vitro* tests (Fig. 4G).

Tuning of trigger sensitivity (e.g., by RBS modulation) is important for generating responses to physiological conditions of interest and for successful application in synthetic engineered circuits. As we observed, RBS tuning can be used to increase the response of the ynfE promoter to as high as 100% in healthy mice (PAS816; Fig. 4F),

and to adjust the response to distinguish the inflamed gut state (PAS819; Fig. 5C). Importantly, the sensors we identify can be used directly in downstream applications with the memory circuit. This provides an engineering advantage over any responsive genetic elements identified through analysis in their native context, for which incorporation into synthetic circuits would routinely require additional optimization.

Inflammation leads to an increase in nitric oxide produced by the host, which generates nitrate in the intestine (27). However, because the ynfE promoter is activated by a decrease in nitrate, our results suggest that DSS-induced inflammation may lead to lower levels of free nitrate available to *E. coli* NGF-1, possibly due to increased local competition for nitrate via respiration by NGF-1 and other *Enterobacteriaceae*. This idea is supported by our observation of increasingly higher NGF-1 bacterial loads in fecal samples of DSS-treated mice (Fig. S4C and S4F), suggesting a bloom of *E. coli*—and potentially other *Enterobacteriaceae* capable of nitrate respiration—correlated with increasing duration of DSS treatment. This is consistent with previous descriptions of *E. coli* experiencing a growth advantage due to anaerobic respiration of host-derived nitrate (27). Thus, we hypothesize that PAS819 responds in DSS-treated mice specifically through sensing inflammation-induced changes in its own microenvironment.

The HTMS enables both the recording of transient signals and the amplification of low-abundance signals through antibiotic selection. These features serve as a useful complement to other techniques, such as meta-transcriptomic or -proteomic studies which capture an instantaneous snapshot of total RNA or protein content. Screening of genome-wide libraries increases the chances of discovery of new, uncharacterized

346 systems, while curating libraries to focus on a subset of sensors can allow greater fine-
347 tuning and increase the chances of identifying a response for the condition of interest.
348 Our use of the *E. coli* NGF-1 strain as a chassis allows robust colonization of the mouse
349 gut without requiring antibiotic maintenance, leading to retention of high bacterial loads
350 and high library complexity in fecal samples even after long periods in the gut.

351 An expanded arsenal of characterized sensors presents opportunities to
352 construct more complex disease-responsive circuits. For instance, the combination of
353 multiple redundant sensors would increase response accuracy under variable *in vivo*
354 conditions, while complementary sensors may allow “fingerprinting” of different disease
355 states. An exciting possibility is the use of more complex logic and signal processing
356 within a single engineered strain, which may sense multiple inputs and produce anti-
357 inflammatory, antimicrobial or other therapeutic proteins only when a precise set of
358 conditions is satisfied (2). Sensors responding differentially based on localization within
359 the intestine may create opportunities for more targeted drug delivery or for the
360 construction of new safety and containment mechanisms—another important
361 consideration in the deployment of engineered organisms.

362 The potential to engineer synthetic circuits into commensal gut bacteria is a
363 promising new approach to the management of intestinal disease. Synthetic biology is
364 just beginning to tap into the evolutionary breadth of capabilities found in natural
365 systems, and our method represents a practical means for expanding the toolkit of
366 useful sensors for *in vivo* application.

367

368 ## MATERIALS AND METHODS

Media, culture conditions. Unless otherwise mentioned, bacterial cultures were grown at 37°C in LB broth or agar (10 g/L NaCl, 5 g/L yeast extract, 10 g/L tryptone). Mixed liquid cultures (i.e., libraries) were grown in LBPS, which contains Peptone Special (Sigma) instead of tryptone. To quantify memory response on indicator plates, agar was supplemented with 60 µg/ml X-gal.

High-throughput memory system (HTMS) construction. The spectinomycin resistance gene, *aadA*, was added downstream of the P_L promoter in the original memory element (9) by overlap extension PCR and genomically integrated by λ Red recombineering (28) into *E. coli* TB10 (29) between *mhpR* and *lacZ*, driving endogenous *lacZ* as a memory-on reporter. From TB10, transfer into streptomycin-resistant *E. coli* NGF-1 was by P1*vir* transduction.

Biosensor strain and library construction. All triggers were cloned into pDR07 (Fig. S2), a Tn7 transposon insertion plasmid derived from pGRG36 (12). BsaI sites directly upstream of cIDN allow modular insertion of promoter–RBS sequences via Golden Gate assembly (13) (Fig. 2A). Assembled trigger plasmids were electroporated into PAS811. After recovery (90 min, 30°C in SOC medium) transformants were selected overnight (30°C in LB-ampicillin (100 µg/ml)). Cultures were then back-diluted 1:100 into LB-chloramphenicol (25 µg/ml) + 0.1% arabinose to induce transposase genes. After > 6 h at 30°C, temperature-sensitive pDR07 plasmids were cured from integrants by 2x 1:100 back-dilution into LB-chloramphenicol and > 6 h growth at 42°C. Plasmid loss was confirmed by restreaking on LB ampicillin agar.

For individual strains, post-cure cultures were plated on LB-chloramphenicol agar and attTn7 integrations confirmed by PCR and Sanger sequencing. For pooled

libraries, library composition was confirmed by Illumina MiSeq sequencing of pooled PCRs of trigger regions.

Assessment of memory state by LacZ assay. Cultures or fecal supernatants containing memory bacteria were plated on agar plates containing streptomycin (200 mg/ml), chloramphenicol (34 mg/ml), and X-gal (60 mg/ml). The percentage of memory-on colonies was assessed by counting blue (on) and white (off) colonies.

***In vitro* induction.** Overnight liquid cultures were back-diluted 1:100 into fresh media containing inducer, before 4 hours growth and plating on X-gal agar. For induction in cecal contents, contents of ceca from three female SPF C57BL/6J mice and suspended at 10% w/v in phospho-buffered saline (PBS). Suspensions were vortexed 90 sec and centrifuged for 3 min at 4300 rcf. The supernatant was recovered, supplemented with 200 μg/ml streptomycin and used for growth of HTMS bacteria.

For anaerobic inductions, pre-reduced anaerobic medium was used, and growth occurred in an anaerobic chamber (Coy Laboratory Products) under 7% H_2, 20% CO_2, 73% N_2.

***In vivo* induction of strains and libraries.** The Harvard Medical School Animal Care and Use Committee approved all animal protocols. Experiments were conducted in female 7- to 14-week-old BALB/c (Charles River; MG1655 library) or C57BL/6J (Jackson; Nissle 1917 library) mice. Before experiments, all mice were confirmed to be absent of native streptomycin- and chloramphenicol-resistant flora. Food and water were removed ~4 h before each gavage; water was replaced immediately, and food was replaced < 2 h following gavage.

One day prior to bacterial gavage, mice were provided streptomycin (20 mg in PBS) by oral gavage. The next day, overnight cultures of memory strains or libraries were washed once, then diluted 10-fold in PBS and administered by gavage (100µl; ~10^7 bacteria/mouse).

Gavage suspension and fecal samples were plated to track bacterial load and, for individual strains, to assess memory state. Libraries were processed according to the post-exposure processing protocol below. To plate fecal bacteria, samples were suspended at 100 mg/ml in PBS, vortexed 5 min, and centrifuged 20 min at 4 rcf to obtain fecal supernatant.

For inflammation experiments, water containing 4% DSS (36,000-50,000 M.W.; MP Biomedicals 160110) was substituted 2 h after bacteria administration. Mice were dissected at the end of the experiment to measure colon length.

Post-exposure library processing. Fecal supernatant or *in vitro* culture was diluted 1:100 into LBPS-chloramphenicol (25 µg/ml) to achieve ~10^6 CFU/ml. Concurrently, an overnight culture of the positive normalization strain, PAS812 was back-diluted 1:100 into LBPS-chloramphenicol. Cultures were grown 4 h, or until OD_{600} ~1. PAS812 OD_{600} was adjusted to match the library culture, then diluted 1:1000 into the library culture. The resulting mix was back-diluted 1:1000 into 50 ml LBPS-chloramphenicol, and immediately split into two 25 ml volumes. Spectinomycin (50 µg/ml) was added to one culture, and both were grown overnight before centrifugation to collect bacterial pellets, which were stored at -80°C.

Library sequencing and odds ratio calculation. Genomic DNA was extracted from frozen cell pellets using a Qiagen DNEasy Blood & Tissue Kit. Using genomic DNA

as a template, trigger regions from HTMS libraries were amplified by PCR and sheared with a Covaris M220 ultrasonicator to 200-600 bp fragments. Sheared products were prepared using the New England Biolabs NEBNext Ultra II Prep Kit and sequenced by Illumina MiSeq.

Raw reads were trimmed using Trimmomatic 0.36 (30) and aligned to a reference file (Data Sets S4 and S5 for MG1655 and Nissle 1917 libraries, respectively) using BWA mem 0.7.8 (31). The number of uniquely-mapped reads for each trigger was counted.

Odds ratio is expressed as $(T_{x\text{-}spect}/PNS_{spect})/(T_x/PNS)$, where T_x and $T_{x\text{-}spect}$ are the number of mapped reads for a particular trigger in the untreated and spectinomycin-treated culture, respectively, and PNS and PNS_{spect} are the number of mapped reads for the positive normalization strain (PAS812) in the untreated and spectinomycin-treated culture, respectively. Triggers with < 5 reads in the gavage suspension were discarded, unless they registered > 20 reads at any subsequent timepoint. For each pair of untreated and spectinomycin-treated cultures (from a single fecal sample), odds ratios were calculated for each trigger with ≥ 5 reads in the untreated culture. Statistical significance was assessed with a one-tailed Fisher's exact test (H_0: odds ratio = 0.02; H_a: odds ratio > 0.02). The odds ratio calculation compares each trigger only with itself (between spectinomycin-treated and untreated cultures), normalizing any sequencing length bias between triggers. It also normalizes to the positive normalization strain (PAS812) in each sample, negating read depth disparities between samples.

ACKNOWLEDGEMENTS

We thank Bryan Hsu, Andrew Verdegaal and Joseph Paulson for helpful discussions. A.D.N. was supported by the National Science Foundation Graduate Research Fellowship (DGE1144152 & DGE1745303). S.N.N. was supported by the Ruth L. Kirschstein Individual Postdoctoral NRSA F32 (F32 DK112640-03). D.T.R. was supported by the Human Frontier Science Program Long-Term Fellowship and the NHMRC/RG Menzies Early Career Fellowship from the Menzies Foundation through the Australian National Health and Medical Research Council.

Author contributions: A.D.N., D.T.R., J.J.B, S.N.N., and P.A.S. designed experiments. A.D.N., S.N.N., J.J.B and D.T.R. constructed libraries. A.D.N., S.N.N., D.T.R, D.T., N.N., M.J.N., and M.C.I. performed in vitro characterization. A.D.N. and D.T.R. performed mouse experiments. A.D.N., J.J.B. and D.T.R. performed and analyzed library sequencing. A.D.N., D.T.R. and P.A.S. wrote the manuscript.

REFERENCES

1. Ozdemir T, Fedorec AJH, Danino T, Barnes CP. 2018. Synthetic Biology and Engineered Live Biotherapeutics: Toward Increasing System Complexity. Cell Syst 7:5–16.

2. Riglar DT, Silver PA. 2018. Engineering bacteria for diagnostic and therapeutic applications. Nat Rev Microbiol 16:214.

3. Riglar DT, Giessen TW, Baym M, Kerns SJ, Niederhuber MJ, Bronson RT, Kotula JW, Gerber GK, Way JC, Silver PA. 2017. Engineered bacteria can function in the mammalian gut long-term as live diagnostics of inflammation. Nat Biotechnol 35:nbt.3879.

4. Daeffler KN-M, Galley JD, Sheth RU, Ortiz-Velez LC, Bibb CO, Shroyer NF, Britton RA, Tabor JJ. 2017. Engineering bacterial thiosulfate and tetrathionate sensors for detecting gut inflammation. Mol Syst Biol 13:923.

5. Mimee M, Nadeau P, Hayward A, Carim S, Flanagan S, Jerger L, Collins J, McDonnell S, Swartwout R, Citorik RJ, Bulović V, Langer R, Traverso G, Chandrakasan AP, Lu TK. 2018. An ingestible bacterial-electronic system to monitor gastrointestinal health. Science 360:915–918.

6. Hwang IY, Koh E, Wong A, March JC, Bentley WE, Lee YS, Chang MW. 2017. Engineered probiotic Escherichia coli can eliminate and prevent Pseudomonas aeruginosa gut infection in animal models. Nat Commun 8:ncomms15028.

492 7. Mao N, Cubillos-Ruiz A, Cameron DE, Collins JJ. 2018. Probiotic strains detect and
493 suppress cholera in mice. Sci Transl Med 10:eaao2586.

494 8. Rediers H, Rainey PB, Vanderleyden J, Mot RD. 2005. Unraveling the Secret Lives
495 of Bacteria: Use of In Vivo Expression Technology and Differential Fluorescence
496 Induction Promoter Traps as Tools for Exploring Niche-Specific Gene Expression.
497 Microbiol Mol Biol Rev 69:217–261.

498 9. Kotula JW, Kerns SJ, Shaket LA, Siraj L, Collins JJ, Way JC, Silver PA. 2014.
499 Programmable bacteria detect and record an environmental signal in the
500 mammalian gut. Proc Natl Acad Sci 111:4838–4843.

501 10. Noman N, Inniss M, Iba H, Way JC. 2016. Pulse Detecting Genetic Circuit – A New
502 Design Approach. PLOS ONE 11:e0167162.

503 11. Gimble FS, Sauer RT. 1985. Mutations in bacteriophage lambda repressor that
504 prevent RecA-mediated cleavage. J Bacteriol 162:147.

505 12. McKenzie GJ, Craig NL. 2006. Fast, easy and efficient: site-specific insertion of
506 transgenes into Enterobacterial chromosomes using Tn7 without need for selection
507 of the insertion event. BMC Microbiol 6:39.

508 13. Engler C, Kandzia R, Marillonnet S. 2008. A One Pot, One Step, Precision Cloning
509 Method with High Throughput Capability. PLOS ONE 3:e3647.

510 14. Mutalik VK, Guimaraes JC, Cambray G, Lam C, Christoffersen MJ, Mai Q-A, Tran
511 AB, Paull M, Keasling JD, Arkin AP, Endy D. 2013. Precise and reliable gene

512 expression via standard transcription and translation initiation elements. Nat
513 Methods 10:354–360.

514 15. Ziesack M, Karrenbelt MAP, Bues J, Schaefer E, Silver P, Way J. 2018.
515 Escherichia coli NGF-1, a Genetically Tractable, Efficiently Colonizing Murine Gut
516 Isolate. Microbiol Resour Announc 7:e01416-18.

517 16. Zaslaver A, Bren A, Ronen M, Itzkovitz S, Kikoin I, Shavit S, Liebermeister W,
518 Surette MG, Alon U. 2006. A comprehensive library of fluorescent transcriptional
519 reporters for Escherichia coli. Nat Methods 3:623–628.

520 17. Hughes ER, Winter MG, Duerkop BA, Spiga L, Furtado de Carvalho T, Zhu W,
521 Gillis CC, Büttner L, Smoot MP, Behrendt CL, Cherry S, Santos RL, Hooper LV,
522 Winter SE. 2017. Microbial Respiration and Formate Oxidation as Metabolic
523 Signatures of Inflammation-Associated Dysbiosis. Cell Host Microbe 21:208–219.

524 18. Winter SE, Lopez CA, Bäumler AJ. 2013. The dynamics of gut-associated microbial
525 communities during inflammation. EMBO Rep 14:319–327.

526 19. Xu M, Busby SJW, Browning DF. 2009. Activation and Repression at the
527 Escherichia coli ynfEFGHI Operon Promoter. J Bacteriol 191:3172–3176.

528 20. Di Luccio E, Elling RA, Wilson DK. 2006. Identification of a novel NADH-specific
529 aldo-keto reductase using sequence and structural homologies. Biochem J
530 400:105–114.

21. Jain R, Yan Y. 2011. Dehydratase mediated 1-propanol production in metabolically engineered Escherichia coli. Microb Cell Factories 10:97.

22. Vogel-Scheel J, Alpert C, Engst W, Loh G, Blaut M. 2010. Requirement of Purine and Pyrimidine Synthesis for Colonization of the Mouse Intestine by Escherichia coli. Appl Environ Microbiol 76:5181–5187.

23. Winkler JD, Garcia C, Olson M, Callaway E, Kao KC. 2014. Evolved Osmotolerant Escherichia coli Mutants Frequently Exhibit Defective *N* -Acetylglucosamine Catabolism and Point Mutations in Cell Shape-Regulating Protein MreB. Appl Environ Microbiol 80:3729–3740.

24. Zhang S, Jiao T, Chen Y, Gao N, Zhang L, Jiang M. 2014. Methylglyoxal Induces Systemic Symptoms of Irritable Bowel Syndrome. PLOS ONE 9:e105307.

25. Jones SA, Gibson T, Maltby RC, Chowdhury FZ, Stewart V, Cohen PS, Conway T. 2011. Anaerobic Respiration of Escherichia coli in the Mouse Intestine. Infect Immun 79:4218–4226.

26. Guymer D, Maillard J, Sargent F. 2009. A genetic analysis of in vivo selenate reduction by Salmonella enterica serovar Typhimurium LT2 and Escherichia coli K12. Arch Microbiol Berl 191:519–28.

27. Winter SE, Winter MG, Xavier MN, Thiennimitr P, Poon V, Keestra AM, Laughlin RC, Gomez G, Wu J, Lawhon SD, Popova IE, Parikh SJ, Adams LG, Tsolis RM, Stewart VJ, Bäumler AJ. 2013. Host-Derived Nitrate Boosts Growth of E. coli in the Inflamed Gut. Science 339:708–711.

552 28. Datsenko KA, Wanner BL. 2000. One-step inactivation of chromosomal genes in
553 Escherichia coli K-12 using PCR products. Proc Natl Acad Sci 97:6640–6645.

554 29. Johnson JE, Lackner LL, Hale CA, de Boer PAJ. 2004. ZipA Is Required for
555 Targeting of DMinC/DicB, but Not DMinC/MinD, Complexes to Septal Ring
556 Assemblies in Escherichia coli. J Bacteriol 186:2418–2429.

557 30. Bolger AM, Lohse M, Usadel B. 2014. Trimmomatic: a flexible trimmer for Illumina
558 sequence data. Bioinforma Oxf Engl 30:2114–2120.

559 31. Li H. 2013. Aligning sequence reads, clone sequences and assembly contigs with
560 BWA-MEM. ArXiv13033997 Q-Bio.

561

562 # TABLES

563 **TABLE 1** Key memory strains used in this study.

Strain	E. coli strain	Memory	Trigger Promoter/RBS	Trigger Gene	Source
PAS132	K-12 MG1655	original	tet	*cro*	(9)
PAS133	NGF-1	original	tet	*cro*	(9)
PAS807	K-12 MG1655	original	tet	*cIDN*	this study
PAS808	NGF-1	original	tet	*cIDN*	this study
PAS809	NGF-1	original	tet	*cIDN*	this study
PAS810	NGF-1	HTMS	tet	*cIDN*	this study
PAS811	NGF-1	HTMS	-	-	this study
PAS812	NGF-1	HTMS	fabR	*cIDN*	this study
PAS813	NGF-1	HTMS	ydiL	*cIDN*	this study
PAS814	NGF-1	HTMS	ydjL	*cIDN*	this study
PAS815	NGF-1	HTMS	-	*cIDN*	this study
PAS816	NGF-1	HTMS	ynfE15	*cIDN*	this study
PAS817	NGF-1	HTMS	yeaRWT	*cIDN*	this study
PAS818	NGF-1	HTMS	ynfEWT	*cIDN*	this study
PAS819	NGF-1	HTMS	ynfE17	*cIDN*	this study

564

FIGURES

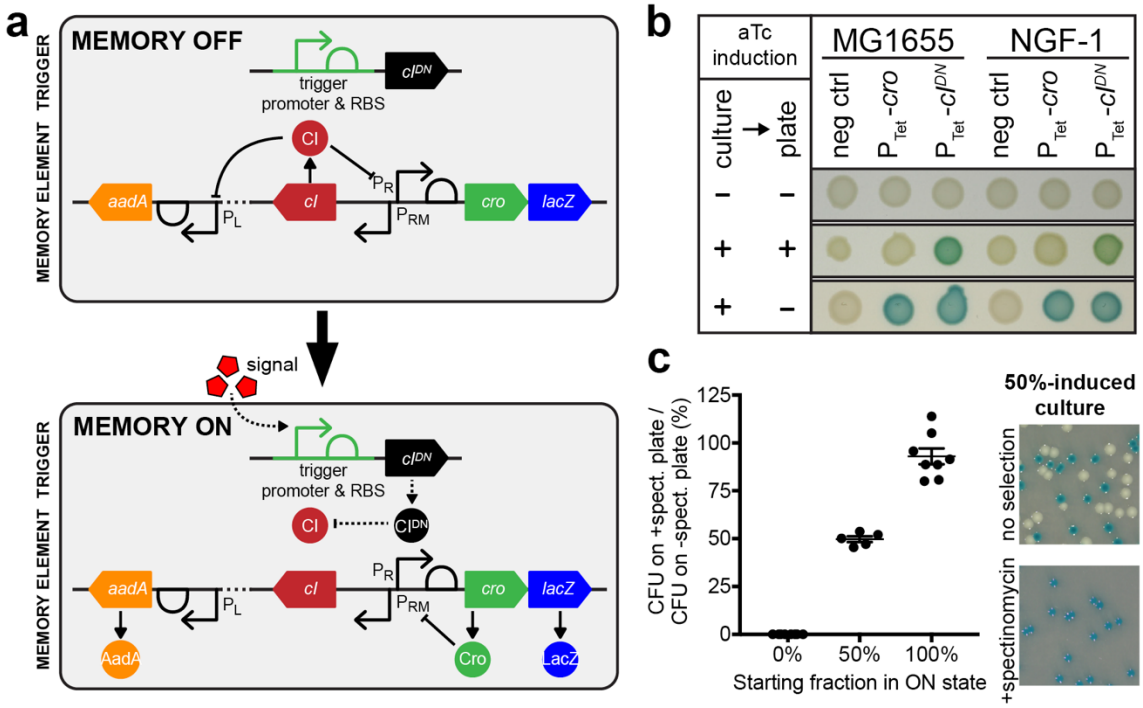

FIG 1 Design of a High-Throughput Memory System (HTMS). (A) HTMS circuit design in memory-off and memory-on states. (B) Comparison of memory element induction with *cro* and *cIDN* triggers illustrates differences in induction dynamics. Control and memory strains with P_{tet} triggers (PAS132, PAS133, PAS807, PAS808) were grown in liquid media, then spotted on indicator plates, each with or without aTc induction (100 ng/ml). (C) Selection of memory-on HTMS with spectinomycin. Memory-off, memory-on, and 50-50 mixed cultures of PAS810 were plated on indicator plates with or without spectinomycin (inset photo). Graph shows comparison of CFU counts between +spectinomycin and -spectinomycin plates. Error bars represent SE of eight biological replicates (for 0% and 100%) and five biological replicates (for 50%).

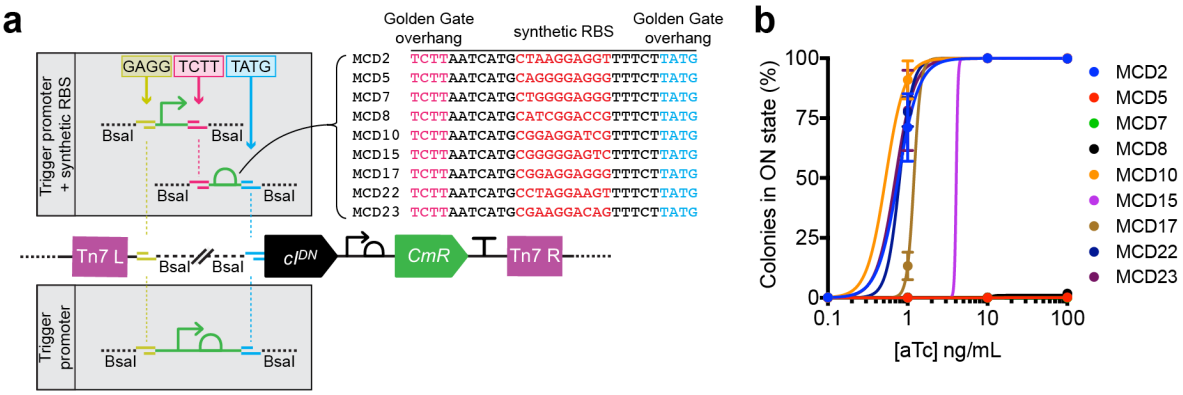

FIG 2 Tuning of trigger sensitivity is achieved through modular incorporation of RBS variants. (A) Strategy for insertion of trigger promoter and RBS variants (14) by Golden Gate assembly (13) into a Tn7 transposon plasmid containing the *cIDN* gene (Fig. S2). (B) Response curves for RBS variants of a Ptet-*cIDN* trigger in the HTMS chassis strain PAS811 induced with varying concentrations of aTc. Memory response was assessed by plating of bacteria on indicator plates after induction with aTc in liquid culture. Error bars represent SE of three biological replicates.

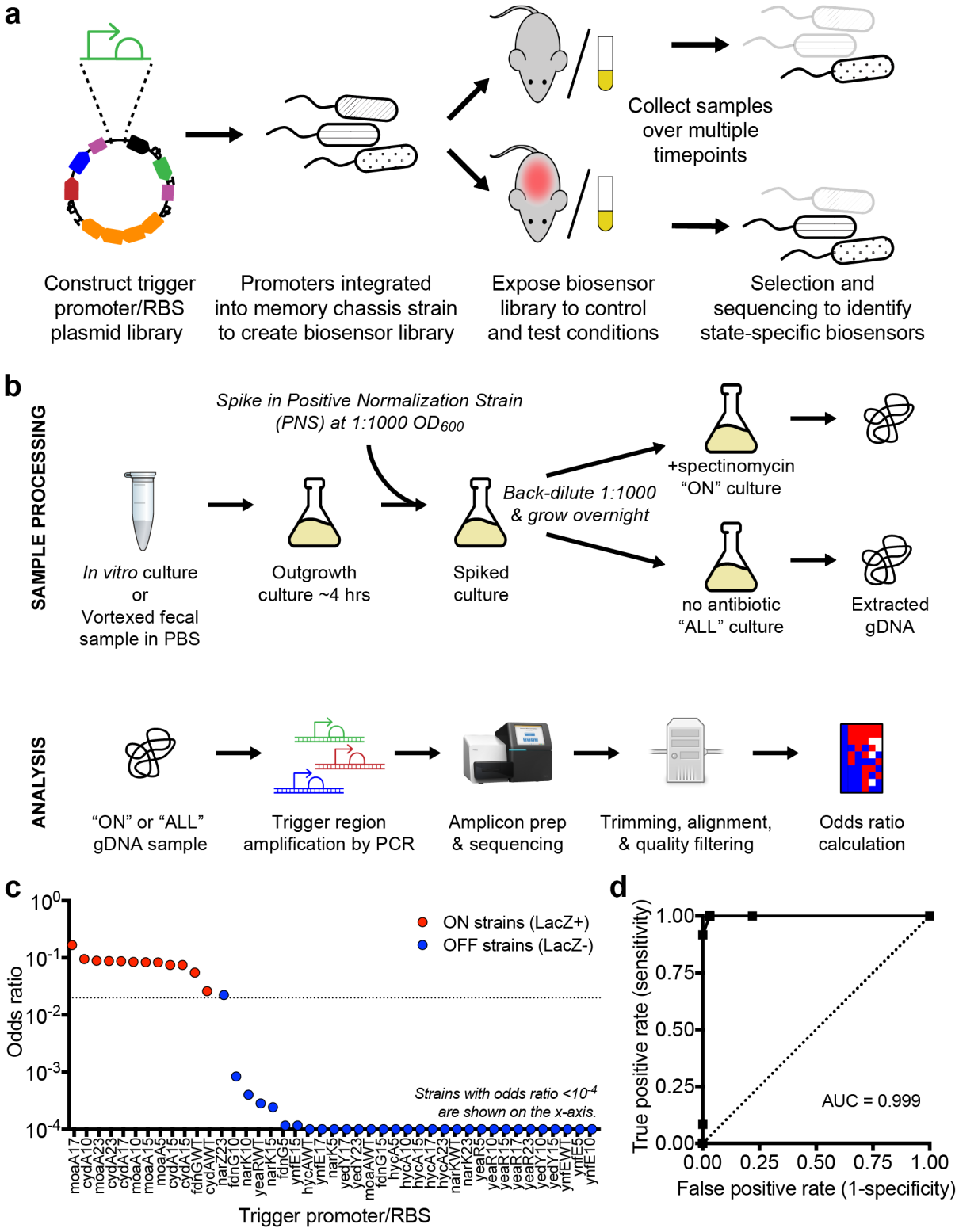

587

588 **FIG 3** Biosensor library screening and analysis. (A) Libraries were constructed as

589 plasmids, integrated into the genome at single copy, and screened as a pool for

590 differential response to growth in control and test environments. (B) Post-exposure
591 library sample processing, selection for memory-on strains, sequencing and analysis.
592 The consistently memory-on positive normalization strain (PAS812) is spiked in prior to
593 spectinomycin selection and used for calculation of odds ratios. (C) Calculated odds
594 ratio from *in vitro* pooled growth in LB medium vs. memory state assessed by plating
595 individual library strains on LB agar indicator plates. 44 strains subsampled from the
596 Nissle 1917 library were tested. The on-off odds ratio cutoff used in the subsequent *in*
597 *vivo* screens (0.02) is indicated by the dotted line. (D) ROC curve for varying odds ratio
598 cutoffs as an indicator of memory state.

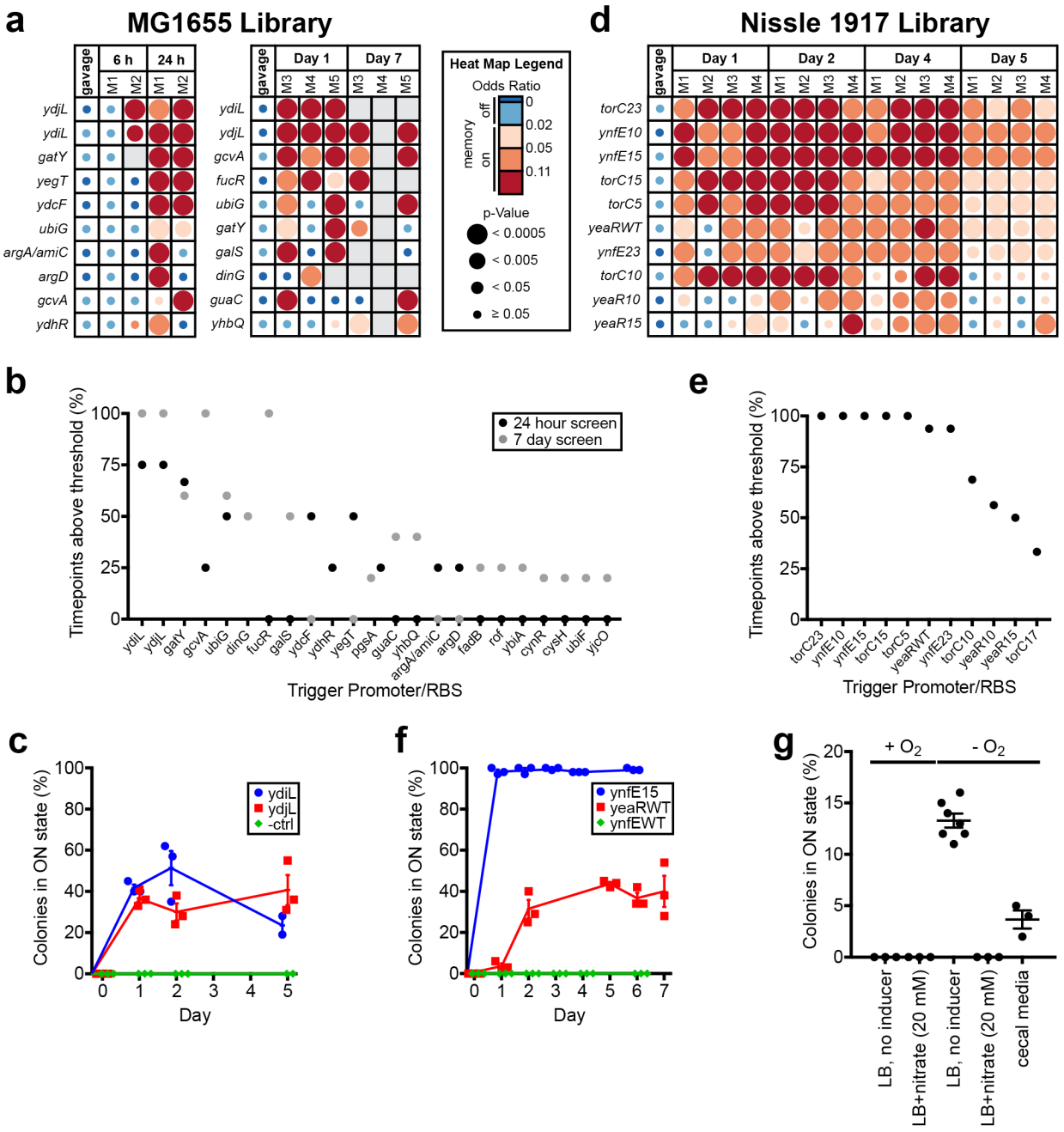

FIG 4 Library screening and individual sensor testing identifies biosensors of the *in vivo* gut environment. (A) Screen of MG1655 library in BALB/c mice over one day (left; n = 2) and over seven days (right; n = 3). Odds ratio heat maps of the top 10 hits sorted by percentage of positive timepoints (odds ratio ≥ 0.02 and $p < 0.05$) over the course of the experiment. Blank spaces on heat maps represent insufficient sequencing coverage.

See Data Set S1 and S2 for full results. (B) Percentage of positive timepoints (odds ratio $\geq$ 0.02 and $p < 0.05$) for all positive hits from two MG1655 library screens (top 10 shown in Fig. 4A). (C) Response of individual strains from MG1655 library in healthy mice. HTMS strains containing triggers ydiL (PAS813), ydjL (PAS814) and an empty trigger (PAS815) were administered as monocultures to BALB/c mice (n = 3). Memory response was assessed by plating of HTMS bacteria recovered from fecal samples on indicator plates. Error bars represent SE. (D) Screen of Nissle 1917 library in C57BL/6J mice (n = 4) over five days. Odds ratio heat map of the top 10 hits sorted by percentage of positive timepoints (odds ratio $\geq$ 0.02 and $p < 0.05$) over the course of the experiment. Blank spaces on heat map represent insufficient sequencing coverage. See Data Set S3 for full results. (E) Percentage of positive timepoints (odds ratio $\geq$ 0.02 and $p < 0.05$) for all hits from Nissle 1917 library screen in healthy mice (top 10 shown in Fig. 4D). (F) Response of individual strains from Nissle 1917 library in healthy mice. HTMS strains containing the ynfE trigger with MCD15 (PAS816), the yeaR trigger with its WT RBS (PAS817) and the ynfE trigger with its WT RBS (PAS818) were administered as monocultures to C57BL/6J mice (n = 3). Memory response was assessed by plating of HTMS bacteria recovered from fecal samples on indicator plates. Error bars represent SE. (G) Response of the ynfE15 trigger strain (PAS816) to *in vitro* growth in rich media with and without 20 mM nitrate, with and without oxygen, and in the presence of mouse cecum fluid medium. Memory response was assessed by plating on indicator plates after growth in liquid culture. Error bars represent SE. (n = 7 for $-O_2$, LB, no inducer condition; n = 3 for all other conditions.)

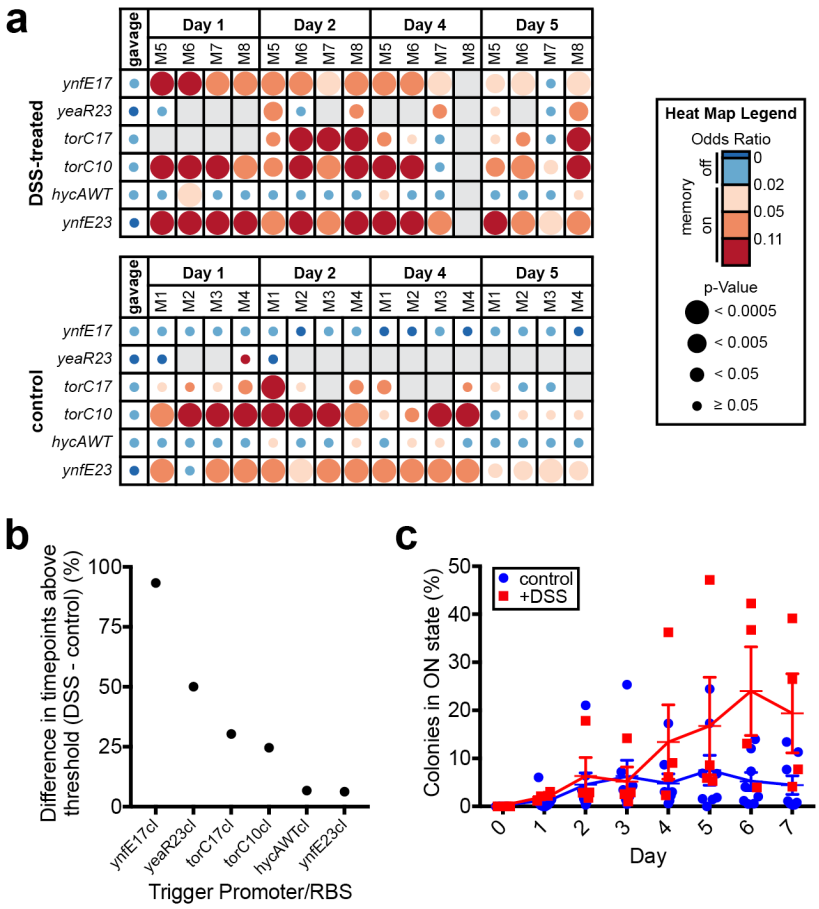

627

628 **FIG 5** Library screening and individual sensor testing identifies biosensors with
629 increased response during inflammation. (A) Screen of Nissle 1917 library in DSS-
630 treated C57BL/6J mice (n = 4) over five days and comparison with results of previous
631 screen in healthy C57BL/6J mice (n = 4; control group; also see Fig. 4D and 4E). To
632 identify sensors responding more strongly to the inflamed state, the fraction of
633 timepoints registering memory-on (odds ratio ≥ 0.02 and $p < 0.05$) in the control group
634 was subtracted from the fraction in the DSS-treated group for each strain in the library,
635 and strains were sorted according to the greatest difference between the two groups.
636 Odds ratio heat map of the six strains registering a positive difference between the two
637 groups is shown. Blank spaces on heat map represent insufficient sequencing
638 coverage. See Data Set S3 for full results. (B) Differences in percentage of positive

timepoints (odds ratio ≥ 0.02 and $p < 0.05$) between DSS-treated and control group mice for strains showing a positive difference between the two groups (heat map shown in Fig. 5A). (C) Response of HTMS strain containing the ynfE trigger with MCD17 (PAS819) in DSS-treated mice (n = 4) and healthy mice (n = 8). Memory response was assessed by plating of HTMS bacteria recovered from fecal samples on indicator plates. Error bars represent SE.

SUPPLEMENTAL MATERIAL LEGENDS

FIG S1 (A) Original memory circuit (9) in memory-off and memory-on states. (B) Response curves of P_{tet}-*cIDN* trigger original memory (PAS809) & an aadA memory strain (PAS810), induced with varying concentrations of aTc. Memory response was assessed by plating on indicator plates after induction with aTc in liquid culture. Error bars represent SE of three biological replicates.

FIG S2 Plasmid map of Tn7 transposon trigger integration plasmid, pDR07, containing BsaI sites upstream of *cIDN* gene for modular insertion of trigger promoter and RBS variants via Golden Gate assembly (see Fig. 2A). Tn7 left and right attachment sites are shown in pink.

FIG S3 Heatmap for hits from Nissle 1917 library screen in healthy C57BL/6J mice (Fig. 4D and 4E), when screened in C57BL/6J mice treated with 4% w/v DSS in water. Blank spaces on heat map represent insufficient sequencing coverage. See Data Set S3 for full heat map.

FIG S4 Body weights, CFU counts, and colon lengths of mice in Nissle 1917 library screen and ynfE17 (PAS819) biosensor strain validation experiments. All error bars represent SE. (A) Percentage of starting body weight for DSS-treated (n = 4) and healthy control (n = 4) mice used in Nissle 1917 library screens. (B) Colon lengths at dissection for DSS-treated (n = 4) and healthy control (n = 4) mice used in Nissle 1917

668 library screens. (C) CFU of HTMS bacteria in fecal samples of DSS-treated (n = 4) and
669 healthy control (n = 4) mice used in Nissle 1917 library screens. (D) Percentage of
670 starting body weight for DSS-treated (n = 4) and healthy control (n = 8) mice used in
671 PAS819 validation experiment. (E) Colon lengths at dissection for DSS-treated (n = 4)
672 and healthy control (n = 8) mice used in PAS819 validation experiment. (F) CFU of
673 HTMS bacteria in fecal samples of DSS-treated (n = 4) and healthy control (n = 8) mice
674 used in PAS819 validation experiment.
675
676 **DATA SET S1.** Screen of MG1655 library in 2 BALB/c mice over 24 hours (full heat
677 map corresponding to Fig. 4A). See Fig. 4 for heat map legend.
678
679 **DATA SET S2.** Screen of MG1655 library in 3 BALB/c mice over seven days (full heat
680 map corresponding to Fig. 4B). See Fig. 4 for heat map legend.
681
682 **DATA SET S3.** Screen of Nissle 1917 library in 8 C57BL/6J mice over five days, with
683 and without DSS treatment (full heat map corresponding to Fig. 4D and 5A). See Fig. 4
684 or Fig. 5 for heat map legend.
685
686 **DATA SET S4.** Sequence reference file (fasta) for aligning MG1655 library reads.
687
688 **DATA SET S5.** Sequence reference file (fasta) for aligning Nissle 1917 library reads.